

University of Groningen

Describing the light intensity dependence of polymer

Slooff, L. H.; Veenstra, S. C.; Kroon, J. M.; Verhees, W.; Koster, L. J. A.; Galagan, Y.

Published in:
Physical Chemistry Chemical Physics

DOI:
[10.1039/c3cp55293d](https://doi.org/10.1039/c3cp55293d)

IMPORTANT NOTE: You are advised to consult the publisher's version (publisher's PDF) if you wish to cite from it. Please check the document version below.

Document Version
Publisher's PDF, also known as Version of record

Publication date:
2014

[Link to publication in University of Groningen/UMCG research database](#)

Citation for published version (APA):

Slooff, L. H., Veenstra, S. C., Kroon, J. M., Verhees, W., Koster, L. J. A., & Galagan, Y. (2014). Describing the light intensity dependence of polymer: fullerene solar cells using an adapted Shockley diode model. *Physical Chemistry Chemical Physics*, 16(12), 5732-5738. <https://doi.org/10.1039/c3cp55293d>

Copyright

Other than for strictly personal use, it is not permitted to download or to forward/distribute the text or part of it without the consent of the author(s) and/or copyright holder(s), unless the work is under an open content license (like Creative Commons).

The publication may also be distributed here under the terms of Article 25fa of the Dutch Copyright Act, indicated by the "Taverne" license. More information can be found on the University of Groningen website: <https://www.rug.nl/library/open-access/self-archiving-pure/taverne-amendment>.

Take-down policy

If you believe that this document breaches copyright please contact us providing details, and we will remove access to the work immediately and investigate your claim.

Downloaded from the University of Groningen/UMCG research database (Pure): <http://www.rug.nl/research/portal>. For technical reasons the number of authors shown on this cover page is limited to 10 maximum.

Describing the light intensity dependence of polymer:fullerene solar cells using an adapted Shockley diode model

Cite this: *Phys. Chem. Chem. Phys.*, 2014, 16, 5732

L. H. Slooff,^{*a} S. C. Veenstra,^{bc} J. M. Kroon,^a W. Verhees,^b L. J. A. Koster^d and Y. Galagan^e

Solar cells are generally optimised for operation under AM1.5 100 mW cm⁻² conditions. This is also typically done for polymer solar cells. However, one of the entry markets for this emerging technology is portable electronics. For this market, the spectral shape and intensity of typical illumination conditions deviate considerably from the standard test conditions (AM1.5, 100 mW cm⁻², at 25 °C). The performance of polymer solar cells is strongly dependent on the intensity and spectral shape of the light source. For this reason the cells should be optimised for the specific application. Here a theoretical model is presented that describes the light intensity dependence of P3HT:[C60]PCBM solar cells. It is based on the Shockley diode equation, combined with a metal–insulator–metal model. In this way the observed light intensity dependence of P3HT:[C60]PCBM solar cells can be described using a 1-diode model, allowing fast optimization of polymer solar cells and module design.

Received 16th December 2013,
Accepted 23rd January 2014

DOI: 10.1039/c3cp55293d

www.rsc.org/pccp

1. Introduction

The power conversion efficiency of polymer solar cells is steadily increasing and has recently reached values of over 10% for size up to 1 cm,^{1,2} increasing the potential of polymer solar cells in different commercial applications. These types of cells will on a short term not be used for large scale applications, but will probably enter the market first as energy generating units in portable devices and cheap electronic devices.

When used in such applications, the polymer solar cells will face different light conditions, both in light intensity and in the spectrum, for example, in indoor applications where the different light sources have different spectral shapes and intensities. As the efficiency of solar cells depends on both light intensity and the spectrum, the design of the cells must be optimized for the specific light conditions that occur for the specific application. This is where modelling can play an important role.

Modelling polymer solar cells has increasingly gained interest in the last decade. Several device physics and optical models have been reported^{3–7} that accurately describe the observed

device performance on the cell level. These models do not take into account the effects of series resistance caused by the metallization and external circuit, and thus describe the intrinsic cell performance. Such device physics and optical modelling can be used to determine the accurate device structure with respect to layer thicknesses in the device. For optimization of the metallization for the electrodes, series resistance effects and shadow loss due to the metallization must be included. Such models have recently been reported by several groups.^{8,9} All these models need intrinsic current–voltage (*IV*) characteristics as inputs, to describe the diode characteristics of the cell. This can be based on an experimental *IV* curve which has been corrected for the series resistance and shadow losses in the measurement, or it can be the result of a device physics model. It has been shown previously for P3HT:[C60]PCBM solar cells¹⁰ that finite element modelling (FEM) is able to describe the performance of cells, using the diode properties or *IV* characteristics of a small cell as input parameters. However, it turned out that this only holds for one light intensity. If a different light intensity is used, new diode properties or *IV* characteristics for that specific light intensity are needed.

For modelling of inorganic solar cells often a 1-diode or the Shockley model¹¹ is used and most of the available or commercial software for solar cells is based on this type of model. The standard Shockley equation is not sufficient to model the operation of polymer solar cells. For this reason the Shockley equation was extended.^{12–15} Although the cells could to a large extent be described using this model, it did not always generate accurate results. Often the light intensity dependence is not

^a ECN Solar Energy, P.O. Box 1, NL-1755 ZG Petten, The Netherlands.
E-mail: slooff@ecn.nl

^b ECN Solar Energy, Energy Research Centre of the Netherlands,
High Tech Campus 5 (P63), 5656AE Eindhoven, The Netherlands

^c Solliance, High Tech Campus 5, 5656AE Eindhoven, The Netherlands

^d Zernike Institute for Advanced Materials, University of Groningen, Nijenborgh 4,
9747 AG Groningen, The Netherlands

^e Holst Centre, High Tech Campus 31, 5656 AE Eindhoven, The Netherlands

correctly described. So in order to model the performance of the intrinsic properties of polymer solar cells, including the light intensity dependence, a sophisticated device physics model is needed but for optimization of the metallization a simple 1-diode model is preferred that enables the use of standard software.

In this paper we combine the 1-diode model with the device physics model for polymer solar cells of the Blom group.⁴ Using this approach we are able to describe the light intensity dependence of various P3HT:[C60]PCBM solar cells. This opens the way for fast optimization of different polymer solar cells and module designs.

2. Experimental

Three series of large area ITO-free organic solar cell devices were prepared. The devices consisted of the following layer stack: current collecting metal grids/high conductivity PEDOT:PSS/P3HT:[C60]PCBM/LiF:Al. The Mo/Al/Mo grids were prepared on glass substrates by sputtering. The thickness of the aluminium layer was 100 nm resulting in Mo/Al/Mo grids with heights (thicknesses) of 10/100/10 nm. The current collecting grids have a pattern of parallel lines with a spacing (pitch) of 2 mm and the width of the lines is 100 μm . Such grids provide 5% of surface coverage. All devices had rectangular shape (see Fig. 1), a width of 2.4 cm and the length between 1 and 6 cm for each series of devices. The devices were prepared on 6 glass substrates and each substrate contained 6 devices with the length from 1 to 6 cm.

High conductivity OrgaconTM PEDOT:PSS from Agfa-Gevaert was inkjet printed on top of substrates with the current collecting grids. For inkjet printing of PEDOT:PSS a Spectra Galaxy 256 print-head was used. The thickness of PEDOT:PSS, with a sheet conductivity of 200 S cm^{-1} , was 100 nm. It provides a sheet resistance for PEDOT:PSS layers of 500 Ωsq^{-1} .

Poly(3-hexylthiophene) (P3HT) (purchased from Plextronics, Plexcore OS 2100) and [6,6]-phenyl-C61-butyric acid methyl ester (PCBM) (99%, purchased from Solenne BV) were dissolved in 1,2-dichlorobenzene with a mixing ratio of 1 : 1 by weight and

a concentration of 2 wt% of each. The solution was stirred for 3 h at 80 $^{\circ}\text{C}$. The photoactive layer was obtained by spin coating the blend at 1000 rpm for 30 seconds, which corresponds to a thickness of 220 nm. The thicknesses of the films were measured using a Dektak profilometer. The experiments were performed in a clean-room environment in an ambient atmosphere. The metal cathode (1 nm LiF, 100 nm Al) was thermally evaporated in a vacuum chamber through a shadow mask. The finished OPV devices were encapsulated with Holst Centre thin film barrier. For each type of solar cells at least 3–5 identical devices were prepared. Current–voltage curves were measured under simulated AM1.5 global solar irradiation (100 mW cm^{-2}), using a WXS-300S-50 solar simulator (WACOM Electric Co.)

3. Finite element model

A finite element model was developed that describes the polymer solar cell.¹⁶ The device is treated as a quasi 2-dimensional system and can be described by the equivalent circuit shown in Fig. 2. At the top in grey are the metal fingers with their resistance, in green is the contact resistance between the metal fingers and the PEDOT:PSS, in purple is the PEDOT:PSS layer with its resistance, in red are the photodiodes of the active layer including shunt resistance and at the bottom in grey is the back contact layer with its resistance.

The active layer is described by a 1-diode equation with its diode parameters, photocurrent density (J_{ph}), dark saturation current density (J_0), the diode ideality factor (n), and shunt resistance (R_{shunt}). The metal grid is coupled to the photo-active layer *via* the contact resistance, whereas the top of the photo-active layer is coupled to the back metal contact *via* the diode properties of the photo-active layer. Iterations are done to make the voltages between the layers consistent. The model calculates the voltage distribution for a certain applied voltage by solving the coupled Poisson equations using a Finite Element Method with a spatial resolution of about 2500 elements per cell.

The model layout can be adapted to suit the specific experimental situation. In this paper two different layouts were used. The layout shown in Fig. 1 and the situation shown in Fig. 3 which shows a cell and its metal contacts as well as the inter-connection from the top contact of one cell to the back contact of the next cell in a module. It is assumed that the ZnO is not contributing to the lateral transport and that its contribution to

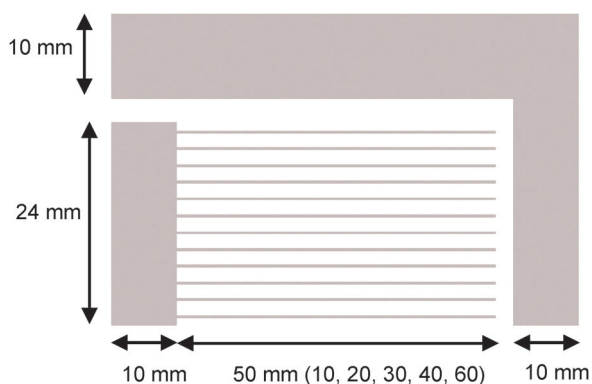


Fig. 1 Schematic presentation of the device layout used in this paper. Grey rectangles indicate the metal contacts and the grey lines the metal fingers of the top contact. Distance between the lines (heart to heart) is 2 mm.

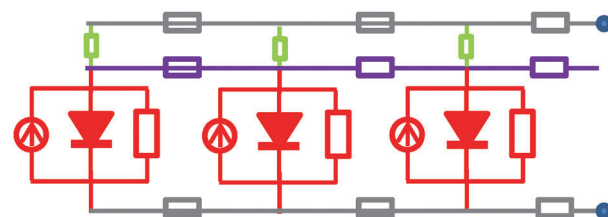


Fig. 2 Schematic drawing showing the equivalent circuit for the model. At the top in grey the top contact, in green the contact resistance between the top contact and the PEDOT layer (purple), the photoactive layer (red part) and at the bottom in grey the back contact.

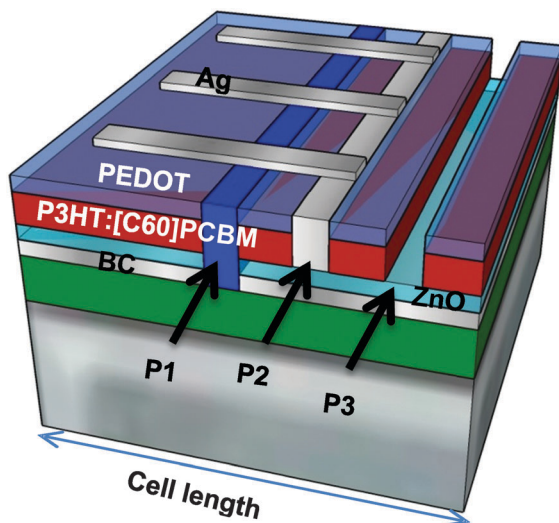


Fig. 3 Schematic drawing of the device structure. Red: active layer, purple: PEDOT layer, light blue bottom: electron transport/hole blocking layer (ETL/HBL), here ZnO; ignored in this calculation, gray bottom: BC back contact, gray top: metal fingers and interconnection. Green: isolation layer. P1: scribe for the isolation between the photoactive layer and the metal of the interconnection, P3 scribe for isolation between the metal of the interconnection and the photoactive layer of the next cell and P2 scribe to open the way for the metal contact between the front side of one cell and back side of the other cell.

the resistance can be neglected. In this paper we refer to the situation shown in Fig. 3 as a single cell module. It is based on monolithic interconnection of individual cells using scribes for the isolation between the photoactive layer and the metal of the interconnection (P1), isolation between the metal of the interconnection and the photoactive layer of the next cell (P3) and to open the way for the metal contact between the front side of one cell and the back side of the other cell (P2).

Furthermore it is assumed that the isolation scribe (P1) is good enough so that there will be no direct current flow between the active layer and the metal of the interconnection. For this reason the isolation and photo-active material between the isolation and the metal of the interconnection were omitted in the model.

4. Results

Current-voltage measurements were performed on cells with different cell lengths and under different illumination intensities. The larger cells will have a larger series resistance than the smaller cells, as the current in the cell is higher and the distances over which the current has to travel before it is collected are larger. It can thus be expected that there will be a voltage distribution in the larger cells due to the series resistance, and as a result not all parts of the cell will be subjected to the same applied voltage. So fitting a large cell to a 1-diode model will not give the intrinsic diode parameters, but effective diode parameters. For this reason we first focused on the smallest, 1 cm cell, as it is expected that the series

resistance for this cell has a negligible influence on the voltage of the cell.

As mentioned in the introduction *IV* curves of inorganic solar cells are often fitted with a generalized Shockley equation:

$$J = J_{\text{ph}} - J_0 \left(e^{\frac{q(V+JR_s)}{nkT}} - 1 \right) + \frac{V + JR_s}{R_{\text{shunt}}} \quad (1)$$

where J_0 is the dark saturation current density, q the elementary charge, R_s the series resistance, V the applied voltage, n the diode ideality factor, k Boltzmann constant, T the temperature, J_{ph} the light induced current density, and R_{shunt} the shunt resistance.

In this work we also fitted the *IV* characteristics of the P3HT:[C60]PCBM cells at different light intensities with eqn (1) in order to determine the series resistance contribution of the 1 cm long cell. Next, the measured *IV* characteristics were corrected for the series resistance and the known shadow losses from the metallization. The resulting *IV*-curve was fitted with the Shockley equation without series resistance.

The resulting diode parameters are shown in Fig. 4, together with a linear fit to the data. As can be seen J_{ph} is linearly dependent on the light intensity, as has been seen before for P3HT:[C60]PCBM cells and which is consistent with the Shockley model. Also $1/R_{\text{shunt}}$ and the ideality factor n show a linear dependence on light intensity. The dependence of the shunt resistance on light intensity has been reported before for polymer solar cells and was attributed to photo-induced recombination events. The light intensity dependence of n is not consistent with the Shockley model which assumes a constant n , and also assumes a constant J_0 with respect to light intensity. But Fig. 4 shows that J_0 increases with light intensity. Clearly, the Shockley model as given in eqn (1) is not able to predict the light intensity dependence of the *J-V* characteristics of P3HT:[C60]PCBM solar cells.

It has been shown before that the light intensity of the V_{oc} for polymer solar cells is accurately described by Koster *et al.* with a model based on a metal-insulator-metal (MIM) model.⁴ The MIM model treats the donor-acceptor blend as an effective semiconductor with the transport of electrons (holes) occurring

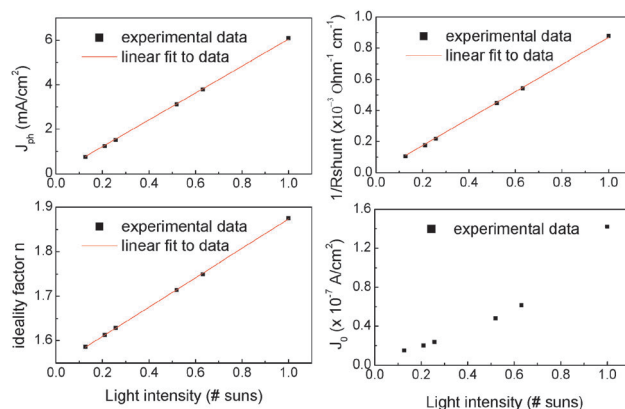


Fig. 4 Measured and fitted relation of J_{ph} , J_0 (no fit), n and $1/R_{\text{shunt}}$ versus light intensity.

in its conduction (valence) band. The expression for the V_{oc} of that model is given by

$$V_{oc} = \frac{E_{gap}}{q} - \frac{kT}{q} \ln \left(\frac{(1-P)k_r N_{CV}^2}{P G_{e-h}} \right) \quad (2)$$

in which E_{gap} is the effective bandgap of the cell (HOMO–LUMO difference), q the elementary charge, P the electron–hole pair dissociation probability, k_r the bimolecular recombination rate, N_{CV} the effective density of states of valence and conduction bands, G_{e-h} the generation rate of bound electron–hole pairs in the photoactive layer (PAL). In eqn (2) only the generation rate of bound electron–hole pairs depends on the light intensity (I_{ill}) and this relation is assumed to be linear:

$G_{e-h}(I_{ill}) = G_{e-h}(1 \text{ sun}) * I_{ill}$. Thus we can rewrite eqn (2) as:

$$V_{oc} = \frac{E_{gap}}{q} - S \frac{kT}{q} \ln \left(\frac{C}{I_{ill}} \right) \quad (3)$$

with

$$C = \frac{(1-P)k_r N_{CV}^2}{P G_{e-h}(1 \text{ sun})} \quad (4)$$

and S times kT/q is the slope of a graph of V_{oc} versus the logarithm of the light intensity as shown in Fig. 5. S depends on the material of the photo-active layer and gives an indication of the type of recombination in the layer.

The equation for the V_{oc} that follows from the Shockley equation is given by

$$V_{oc} = \frac{nkT}{q} \ln \left(\frac{J_{ph}}{J_0} + 1 \right) \quad (5)$$

To incorporate the MIM model into the Shockley equation the V_{oc} of eqn (3) is kept equal to the V_{oc} of eqn (5). By solving this equation for J_0 , an expression for J_0 can be found that is consistent with the MIM model:

$$J_0 = \frac{J_{ph}}{e^{\left(\frac{E_{gap}}{nkT} - \frac{1.25}{n} \ln \left(\frac{C}{I_{ill}} \right) \right)} - 1} \quad (6)$$

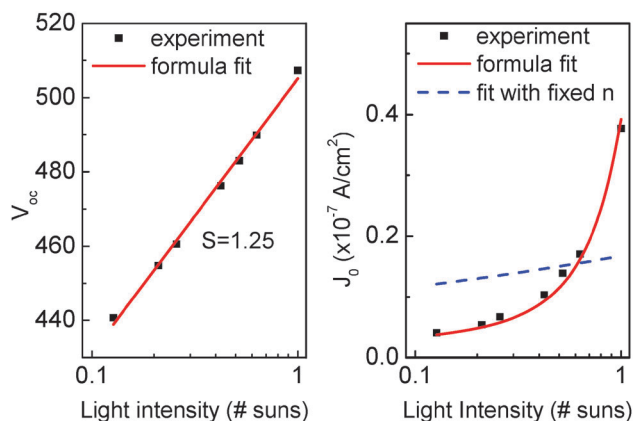


Fig. 5 Left: measured light intensity dependence of V_{oc} (black squares) and a fit of eqn (3) to the data (red line). Right: measured J_0 (black squares) and a fit to the data using eqn (6) (red line).

where a value of 1.25 was taken for S as was determined previously for P3HT:[C60]PCBM.^{17,18}

The measured V_{oc} and J_0 as a function of light intensity were fitted with eqn (3) and (6) respectively. For the fit the measured linear intensity dependencies of J_{ph} and n as shown in Fig. 4 were used and a literature value of 1.0 eV was taken for E_{gap} . Only parameter C was fitted. The results are shown in Fig. 5.

As can be seen, both V_{oc} and J_0 are very well described by their respective formulas, when using the linear light intensity dependencies of n and J_{ph} . The dashed line in the J_0 graph indicates the result when a constant n is taken. Clearly this does not match the experimentally observed light intensity dependence of J_0 . The value of C that results from the fit of the V_{oc} is 5.0×10^6 . For the J_0 fit a value of 4.0×10^6 is found for C . These values are close to the value of 5.8×10^6 for C that is obtained when using the literature values of Table 1 in eqn (5). The difference may lie in the uncertainty of the literature values but also the cells used in this work might have a somewhat different morphology leading to slightly different values.

So the light intensity dependence of the P3HT:[C60]PCBM cells can be explained by the observed linear dependencies of J_{ph} , R_{sh} and n , and the derived relation for J_0 . The question that remains is, why is n depending on light intensity?

It is known that the current in polymer solar cells can be described by

$$J = qL(G - L) \quad (7)$$

In which L is the layer thickness, G is the generation term and R is the recombination term. The latter contains recombination between injected (dark) carriers, photogenerated carriers, and their cross-terms and is given by

$$R = k_r [(n_d + n_{ph})(p_d + p_{ph})] \quad (8)$$

Substitution of eqn (8) into eqn (7) gives

$$\begin{aligned} J &= qGL - k_r(n_d p_d + n_{ph} p_{ph} + n_{ph} p_d + n_d p_{ph}) \\ &= J_{ph} - k_r n_d p_d - k_r(n_{ph} p_{ph} + n_{ph} p_d + n_d p_{ph}) \end{aligned} \quad (9)$$

in which n_{ph} (p_{ph}) are the photogenerated electron (hole) densities, and n_d (p_d) are the dark electron (hole) densities.

The first term, qGL , is the photocurrent and is equal to the J_{ph} in eqn (1). The second term is similar to the second term in eqn (1) as it describes the injection of dark carriers.

So only if the terms in the third term are negligible, the superposition of photo- and dark current, as assumed in the

Table 1 Literature values for parameters for P3HT:PCBM solar cells

Parameter	Value	Ref.
k_r	$6 \times 10^{-18} \text{ s}^{-1}$	19
N_{CV}	$2.5 \times 10^{26} \text{ m}^{-3}$	4
E_{gap}	$1.602 \times 10^{-19} \text{ J (1 eV)}$	20
P	0.9	16
G_{e-h}	(at 0.8 suns) $5.7 \times 10^{27} \text{ m}^{-3} \text{ s}^{-1}$	21
T	293 K	

Shockley equation, holds (we ignore here the contribution of the shunt resistance, as this is similar in both models). In general however, in polymer solar cells the photo-recombination terms will not be negligible, resulting in a deviation from the Shockley equation. The cross terms depend on intensity. The $n_{ph}n_{ph}$ term is quadratically dependent on light intensity as it depends on the square of photogenerated carrier densities, whereas the other terms depend linearly on light intensity. So the question is, can the Shockley equation be written with the intensity dependent parameters such that it resembles the intensity dependence of eqn (9), *i.e.*

$$J = J_{ph}(I_{ll}) - J_0(I_{ll}) \left(e^{\frac{qV}{n(I_{ll})kT}} - 1 \right) \quad (10)$$

$$= J_{ph}(I_{ll}) - \gamma(a \times I_{ll}^2 + b \times I_{ll} + c)$$

with $J_0(I_{ll})$ from eqn (6) and $n = n_1 + n_2 \times I_{ll}$. First the expression for J_0 and n was inserted in the left side of eqn (10) and a second order Taylor series around $I_{ll} = 1$ was performed. Next the third order term was ignored and the constant terms, the terms linear with I_{ll} and the terms quadratic in I_{ll} , were collected. The expressions for the constants a , b and c are too large to display them in this paper, but using these expressions the current density could indeed be expressed in terms of I_{ll} and I_{ll}^2 similar to the right side of eqn (10). To show the validity of the result, Fig. 6 shows the measured J - V curves at 2 different intensities together with the calculated result based on the Taylor series. As can be seen, the calculated curves nicely overlap the experimental curves.

Another difference between organic and inorganic cells is the field dependence of the photogenerated current density in polymer solar cells as shown by Mihailetchi *et al.*²² for P3HT:[C60]PCBM solar cells. They showed very good agreement between experimental results and the calculated J_{ph} as a function of the effective applied voltage ($V_0 - V$) using their device physics model including the field- and temperature-dependent generation rate $G(E, T)$. This field dependence is typically plotted as J_{ph} versus the effective applied voltage $V_0 - V$, where V_0 is the voltage at $J_{ph} = 0$. J_{ph} is then determined as the current density under illumination plus the current density in the dark:

$$J_{ph}(V, I_{ll}) = J + J_{dark} \quad (11)$$

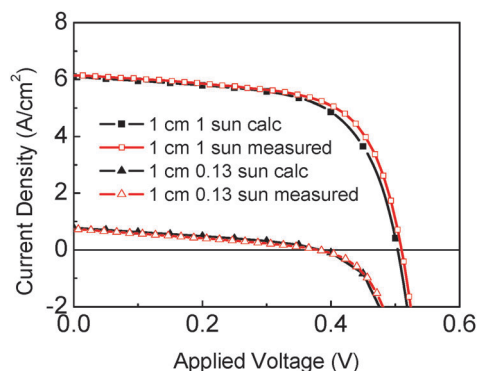


Fig. 6 Calculated and experimental J - V curves for two different illumination intensities.

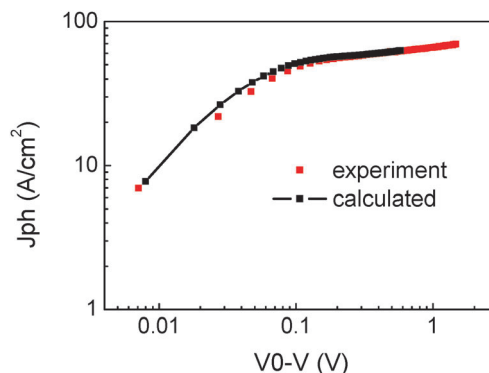


Fig. 7 Photon current density as function of the effective applied voltage for a 1 cm long cell at an illumination intensity of 1 sun. In red the experimental results, in black the calculation result using $J_{ph} = J_{ph} - c$.

Substitution of eqn (10) gives:

$$J_{ph}(V, I_{ll}) = J_{ph}(I_{ll}) - J_0(I_{ll}) \left(e^{\frac{qV}{n(I_{ll})kT}} - 1 \right) + J_0(0) \left(e^{\frac{qV}{n(0)kT}} - 1 \right) \quad (12)$$

$$= J_{ph}(I_{ll}) - \gamma(a \times I_{ll}^2 + b \times I_{ll} + c) + J_0(0) \left(e^{\frac{qV}{n(0)kT}} - 1 \right)$$

From eqn (12) it can be seen that $J_{ph}(V, I_{ll}) \neq J_{ph}(I_{ll})$ because $J_0(I_{ll}) \neq J_0(0)$ and $n(I_{ll}) \neq n(0)$. So only if J_0 and n would be constant with light intensity, J_{ph} would be field independent. Fig. 7 shows the experimental $J_{ph}(V, I_{ll})$ versus $V_0 - V$ together with the calculated $J_{ph}(V, I_{ll})$ from eqn (12). Again a good agreement between experiment and calculation is found.

These results show that by adapting the diode parameters in the Shockley diode model such that they represent the MIM model, very good agreement is found between the model and experiments.

The light intensity dependencies were implemented in two models, an analytical model, that assumes that every part of the cell is subjected to the same voltage, and a distributed series resistance model as described by the FEM model above. The results are shown in Fig. 8 for different light intensities and finger lengths of 1 cm and 6 cm.

As can be seen, the analytical model shows good agreement for the cell with fingers of 1 cm length, although the model starts to overestimate the FF and P_{mpp} for higher light intensities. This indicates that for such a short cell the series resistance does not result in a significant lateral voltage drop at low light intensities, but that series resistance effects reduce the power conversion efficiency under 1 sun conditions. The series resistance gives rise to a voltage drop over the cell which will at first affect the FF of the device. The FF for the short cell remains above 60%, having no influence on J_{sc} . However, for the long cell the FF drops much faster due to the higher current densities in this cell. Already at light intensities slightly

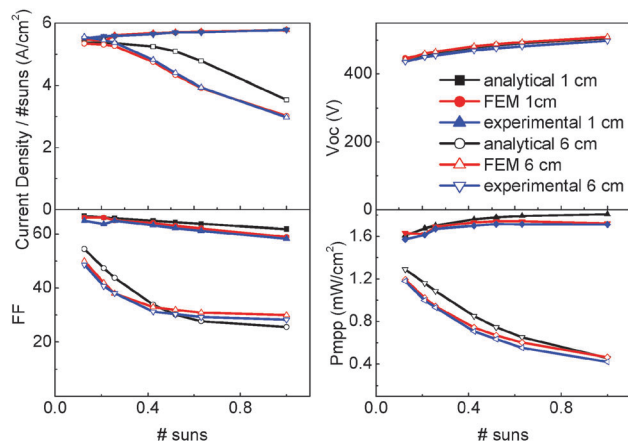


Fig. 8 IV-parameters as function of illumination intensity for a cell with a finger length of 1 cm and 6 cm. Shown are the calculation results for an analytical model (black), FEM model (red) and experimental results.

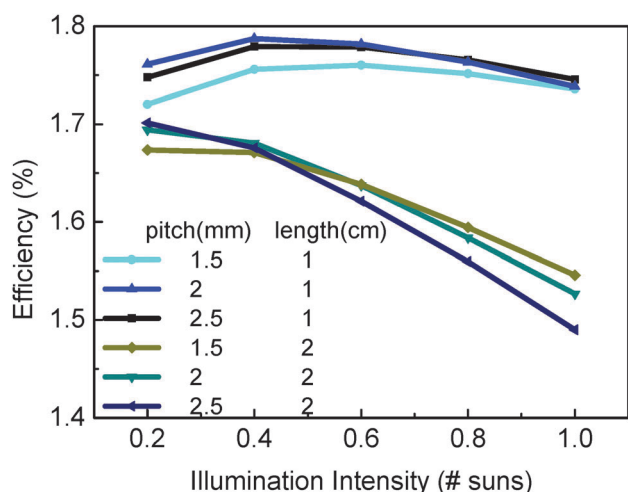


Fig. 9 Efficiency versus illumination intensity for 1 and 2 cm long cells with 1.5, 2 or 2.5 mm pitch.

over 0.3 sun, the FF drops below 40% and starts to affect the J_{sc} . The analytical model is not able to explain the behaviour of the FF and J_{sc} for the long cell at higher light intensities. The assumption that the whole cell is facing the same applied voltage clearly does not hold under these conditions. The voltage drop is

so large that part of the cell is operating at V_{oc} or even further, reducing the current density substantially. The FEM model on the other hand shows excellent agreement with the measured J_{sc} , showing that the model is able to predict both the light intensity dependence and the effect of the distributed series resistance. For these large cells an analytical model is not sufficient to give an accurate estimate of the performance and a FEM model should be used.

The FEM model including the light intensity dependence of the cells can be used to determine the optimum grid geometry for various light intensities. This is shown in Fig. 9 where the efficiency of the total area is plotted for light intensities varying from 0.2 to 1 sun, for cell lengths of 1 and 2 cm and pitches of 1.5, 2 and 2.5 mm. Table 2 gives the values for the diode parameters that were used in the calculation and Table 3 the values for the other parameters in the model.

For the 1 cm long device, the efficiency first increases with light intensity and then decreases for all pitches. Increasing the light intensity results in an increase in current density, which causes a decrease in the fill factor due to resistive losses. On the other hand, the V_{oc} will increase with light intensity. These opposing mechanisms result in an optimum in efficiency around 0.5 sun. Increasing the cell length to 2 cm shifts the optimum to lower illumination intensity, as the resistive losses become larger, whereas the dependence of the V_{oc} on light intensity remains the same. Fig. 9 also shows that the pitch can be optimized for light intensity. For the 2 cm long cell, the optimum pitch at 0.2 sun is 2.5 mm, whereas at 1 sun it is 1.5 mm. This clearly shows the need for optimization of grid patterns for different illumination intensities.

Table 3 Parameter values used for the calculations

Parameter	Value
Sheet resistance metal (Ohm sq)	0.24 (= $3 \times$ bulk)
Sheet resistance back contact (Ohm sq)	0.24 (= $3 \times$ bulk)
Contact resistance finger/PEDOT (Ohm cm^2)	0.005
Contact resistance in interconnect (Ohm cm^2)	0.01
Rsheets pedot (Ohm sq)	249.676
Thickness lines, back contact (μm)	0.2
Fingerwidth (cm)	0.01
Scribe widths (cm)	0.002
Distance between the scribes (cm)	0.01
Distance between end finger and PEDOT (cm)	0.018

Table 2 Values for light intensity dependence of P3HT:[C60]PCBM diode parameters

Parameter	Description	Value
J_{pho}	Photon current density at 1 sun light intensity (mA cm^{-2})	6.135
I_{light}	Light intensity (number of suns)	0.13–1.0
n_{low}	Diode ideality factor at low light intensity	1.431
n_{high}	Diode ideality factor at high light intensity	1.673
Int_{high}	Light intensity at high light intensity (number of suns)	1.0
Int_{low}	Light intensity at low light intensity (number of suns)	0.13
E_{gap}	Bandgap energy	1.0
T	Temperature (K)	298.15
C	Fitting constant	3.9×10^6
$R_{shuntlow}$	Shunt resistance at low light intensity (Ohm cm^2)	689.988
$R_{shunthigh}$	Shunt resistance at high light intensity (Ohm cm^2)	6429.628

5. Conclusions

Here a model is described that is able to simulate the light intensity behaviour of P3HT:[C60]PCBM solar cells. The model is based on the Shockley diode model, but it includes light intensity dependencies of J_0 , n , and R_{shunt} . The dependencies are determined from a 1-diode model fit to measured IV curves, one at low light intensity and one at roughly 1 sun light intensity. A linear fit to n and $1/R_{\text{shunt}}$ versus light intensity gives the dependencies of n and R_{shunt} . For J_0 a formula is derived using the expression of the V_{oc} for polymer solar cells from Koster *et al.* This formula is based on material constants that have been derived previously for P3HT:[C60]PCBM solar cells. Using this approach the voltage dependence of the photon current density could also be described. The dependencies were implemented in a FEM model and show excellent agreement with experimental results for all light intensities and both short and long cells. This model was then used to show that the optimal pitch of a metal grid depends on the illumination intensity.

This opens the way for fast optimization of polymer solar cells and modules for different applications, performing under different light intensities.

Acknowledgements

This work has been supported by the European Commission as part of Framework 7 ICT collaborative projects HIFLEX (Grant no. 248678), X10D (Grant no. 287818) and Dutch ministry of economic affairs through the EOS-LT program (agreement number: EOS LT 10023), the OZOFAB project.

References

- 1 M. A. Green, K. Emery, Y. Hishikawa, W. Warta and E. D. Dunlop, *Prog. Photovolt. Res. Appl.*, 2012, **20**, 606–614.
- 2 R. F. Service, *Science*, 2011, **332**, 293–303.
- 3 P. Schillinsky and C. Waldauf, *J. Appl. Phys.*, 2004, **95**, 2816–2819.
- 4 L. J. A. Koster, E. C. P. Smits, V. D. Mihailetschi and P. W. M. Blom, *Phys. Rev. B: Condens. Matter Mater. Phys.*, 2005, **72**, 085205.
- 5 R. Häusermann, E. Knapp, M. Moos, N. A. reinke, T. Flatz and B. Ruhstaller, *J. Appl. Phys.*, 2009, **106**, 104507.
- 6 G.-J. A. H. Wetzelaer, M. Kuik, M. Lenes and P. W. M. Blom, *Appl. Phys. Lett.*, 2011, **99**, 153506.
- 7 G.-J. A. H. Wetzelaer, M. Kuik and P. W. M. Blom, *Adv. Energy Mater.*, 2012, **2**, 1232–1237.
- 8 Y. Galagan, B. Zimmermann, E. W. C. Coenen, M. Jørgensen, D. M. Tanenbaum, F. C. Krebs, H. Gorter, S. Sabik, L. H. Slooff, S. C. Veenstra, J. M. Kroon and R. Andriessen, *Adv. Energy Mater.*, 2012, **2**, 103–110.
- 9 B. Kippelen, S. Choi and W. J. Potscavage, 10th Int. Conf. NUSOD, 2010, 67–68.
- 10 Y. Galagan, E. W. C. Coenen, B. Zimmermann, L. H. Slooff, W. J. H. Verhees, S. C. Veenstra, J. M. Kroon, M. Jørgensen, F. C. Krebs and R. Andriessen, *Adv. Energy Mater.*, 2014, **4**, DOI: 10.1002/aenm.201300498.
- 11 W. Shockley, *Bell System Tech. J.*, 1949, **28**, 435–489.
- 12 V. Dyakonov, *Appl. Phys. A: Mater. Sci. Process.*, 2004, **79**, 21–25.
- 13 W. J. Potscavage, S. Yoo and B. Kippelen, *Appl. Phys. Lett.*, 2008, **93**, 193308.
- 14 B. P. Rand, D. P. Burk and S. R. Forrest, *Phys. Rev. B: Condens. Matter Mater. Phys.*, 2007, **75**, 115327.
- 15 N. Li, B. E. Lassiter, R. R. Lunt, G. Wei and S. R. Forrest, *Appl. Phys. Lett.*, 2009, **94**, 023307.
- 16 L. H. Slooff, A. R. Burgers, E. E. Bende, S. C. Veenstra and J. M. Kroon, *Proc. 28th EU-PVSEC*, 2013, 2776–2780.
- 17 G.-J. A. H. Wetzelaer, M. Kuik and P. W. M. Blom, *Adv. Energy Mater.*, 2012, **2**, 1232–1237.
- 18 M. Lenes, S. W. Shelton, A. B. Sieval, D. F. Kronholm, J. C. Hummelen and P. W. M. Blom, *Adv. Energy Mater.*, 2009, **19**, 3002.
- 19 V. D. Mihailetschi, L. J. A. Koster, J. C. Hummelen and P. W. M. Blom, *Phys. Rev. Lett.*, 2004, **93**, 216601.
- 20 G. A. H. Wetzelaer, N. J. van der Kaap, L. J. A. Koster and P. W. M. Blom, *Adv. Energy Mater.*, 2013, **3**, 1130.
- 21 L. J. A. Koster, PhD thesis, University of Groningen, 2007, p. 92.
- 22 V. D. Mihailetschi, H. Xie, B. de Boer, L. J. A. Koster and P. W. M. Blom, *Adv. Funct. Mater.*, 2006, **16**, 699–708.